POLITECNICO DI TORINO
Repository ISTITUZIONALE

Probabilistic Assessment of Windblown Sand Accumulation Around Railways

Original
Probabilistic Assessment of Windblown Sand Accumulation Around Railways / Raffaele, Lorenzo; Bruno, Luca. - ELETTRONICO. - 27:(2019), pp. 562-572. (Intervento presentato al convegno XV Conference of the Italian Association for Wind Engineering tenutosi a Napoli (IT) nel 9-12 settembre) [10.1007/978-3-030-12815-9_43].

Availability:
This version is available at: 11583/2709752 since: 2020-02-27T11:34:51Z

Publisher:
Springer

Published
DOI:10.1007/978-3-030-12815-9_43

Terms of use:

This article is made available under terms and conditions as specified in the corresponding bibliographic description in the repository

Publisher copyright

(Article begins on next page)

13 March 2024

Noname manuscript No.
(will be inserted by the editor)

Probabilistic assessment of windblown sand accumulation around railways

Lorenzo Raffaele · Luca Bruno

Received: date / Accepted: date

Abstract New ultra-long transnational railway megaprojects are currently being planned or under construction. Along their route, they increasingly cross arid and desert regions. In these regions, railways are vulnerable to windblown sand. Several failure cases recently occurred, e.g. along the Linhai-Ceke railway in China, or the Aus-Lüderitz railway in Namibia. We consider windblown sand as an environmental key factor, analogously to wind or snow drift. We categorize its effects into Sand Ultimate Limit States and Sand Serviceability Limit States. In the design perspective, the quantitative prediction of the windblown sand sedimented along the railway is mandatory. We propose a probabilistic approach to sedimented windblown sand modelling because of the inborn variability of the phenomenon. The proposed method allows evaluating the design value of the accumulated windblown sand volume for a given site.

Keywords Windblown sand · sand limit states · railway · Monte Carlo

1 Introduction

Railway megaprojects traditionally includes long and ultra-long railway projects that are characterized by long-lasting impact on the economy, the environment, and society. Some historic examples are the Pacific Railroad (3.100 km, 1863-1869) in North America, and the Trans-Siberian Railway (9.200 km,

Lorenzo Raffaele
Department of Architecture and Design (DAD), Politecnico di Torino
Viale Mattioli 39, 10125, Torino (Italy) E-mail: lorenzo.raffaele@polito.it
Windblown Sand Modeling and Mitigation joint research group (Italy, France)

Luca Bruno
Department of Architecture and Design (DAD), Politecnico di Torino
Viale Mattioli 39, 10125, Torino (Italy) E-mail: luca.bruno@polito.it
Windblown Sand Modeling and Mitigation joint research group (Italy, France)

Fig. 1 Built and planned railway lines in arid and desert regions

1891-1916) in Asia. New ultra-long transnational railway megaprojects are currently being planned (Fig. 1). The Arab League Countries have recently conceived the Arab Network Railway, a 30.000 km long, high-speed/high-capacity railway network across Middle East and North Africa. The Countries of the Gulf Co-operation Council are building the Gulf Railway, a 2.217 km long railway network. The Trans-Asian Railway Southern Corridor, within the broader Iron Silk Road plan, is a 8.000 km long transcontinental network between Europe and Southeast Asia. The corresponding investments are significant: for instance, the Middle East Countries have allocated about USD 260 billion to build 40.000 km of railway tracks up to 2030. Given the extension of their route, railway megaprojects cross different environments, and are subjected to related specific environmental actions. The sand blown by the wind is the most important specific key environmental factor that affects the design of railways crossing arid and desert regions.

Windblown sand induced effects on railways range from construction delays to service suspension and train derailment. They result in expensive track maintenance and sedimented sand removal. In order to mitigate windblown sand effects, a number of windblown Sand Mitigation Measures (SMMs) have been proposed in the last decade. SMMs generally aim at avoiding sand sedimentation on the railway track. In particular, the so-called Path-SMMs [1] promote sand sedimentation away from the railway. Path SMMs mostly translate into barriers located between the sand source and the railway.

Despite pioneering ad-hoc studies for specific projects, a systematic and comprehensive problem setting is still missing. As a consequence, the design, analysis and performance assessment of SMMs remain in the realm of qualitative empiricism. In this study, windblown sand effects are categorized by the resulting level of performance of the railway, and by corresponding sand limit states. Then, we propose a probabilistic approach to windblown sand sedimented around railways because of the inborn variability of both wind and sand characteristics. The proposed method is applied to a case study in the Arabic peninsula.

Fig. 2 Sand Ultimate Limit States: full coverage by encroaching sand dune (a, explicit publishing permission from the owner of the photo Giles Wiggs), partial coverage in a sandy plain (b), jammed turnout (c), train derailment (d, reprinted from [6] with the permission from the editor).

2 Windblown Sand Limit States

Windblown Sand Limit States (SLSs) are defined as threshold performance levels, beyond which the infrastructure no longer fulfils its design criteria. SLSs are separated into Sand Ultimate Limit States (SULSs) and Sand Serviceability Limit States (SSLSs), analogously to safety formats widespread in Civil Engineering [2]. Attaining SULS involves service interruption and/or passengers unsafe conditions. Attaining SSLS involves railway partial loss of capacity and/or passenger discomfort. SLS may be attained by one or more components of the railway infrastructure, e.g. civil works, track superstructure, signalling system, rolling stock. Some SLSs are described in the following. They are fully reviewed in [3].

SULSs are mainly induced by civil works, when the railway embankment or cutting are buried by sedimented sand. This schematically occurs under two different environmental conditions. First, when a field of migrating dunes overruns the alignment (Fig. 2a). Secondly, when the line crosses a sandy plane [4]: the overall railway body acts as an obstacle to the incoming wind flow; it induces the deceleration of the flow around it, and the sand sedimentation in turn (Fig. 2b). SULSs are attained when the full or partial coverage compromises the infrastructure safety or operation. Once civil works attains SULS, SULS can also be attained by the track superstructure. For instance, the sedimented sand may jam railroad switches, analogously to snow and ice in cold environments (Fig. 2c). Service interruption necessarily follows, since switches malfunction leads to train derailment or collision. The full coverage of current segments induces the SULS of rolling stock, i.e. running train derailment [5] (Fig. 2d).

Under SSLSs, windblown sand affects only a single component of the railway. However, this can reverberate on the overall railway system performances, i.e. its speed [7]. The sole SSLS attained by civil works is the partial obstruction of culverts by sedimented sand (Fig. 3e). Among track superstructure SSLS, the most common one is ballast contamination (Fig. 2a-c). It is generally quantified by referring to a permitted level of contamination, quantitatively expressed by the Percentage Void Contamination (PVC). In particular, an allowable limit of PVC is set to 30% for a concrete sleeper track with a 250 mm thick ballast layer [8]. Ballast contamination leads to a series of side effects,

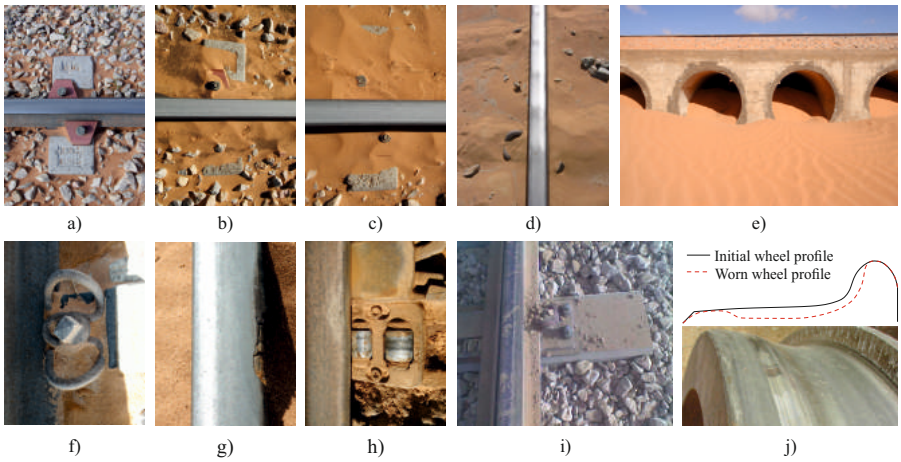

Fig. 3 Sand Serviceability Limit States: different levels of ballast contamination (a-c), rail corrugation (d, reprinted from [12] with the permission from Elsevier), culverts obstruction (e), contamination of fasteners (f), rail head corrosion (g, courtesy of Astaldi), contamination of turnout components (h), downwind rail head (i, courtesy of Astaldi), wheel profiling (j, reprinted from [13] with the permission from Voestalpine).

e.g. increasing of the stiffness and decreasing of the damping of ballast bed and rail support modulus [9], accumulation of permanent deformation, rail corrugation (Fig. 3d). Other examples of track superstructure SSLSs are corrosion and degradation of fastening systems (Fig. 3f), r.c. sleeper and rail (Fig. 3g) due to the salt content of the sand [10]. Furthermore the sand induces abrasive wear inside switches components (Fig. 3h), while the thin layer of sedimented sand on the wheel-rail contract surface leads to rail grinding [11] (Fig. 3i), and rolling stock wheel profiling (Fig. 3j).

The metric describing windblown sand effects and resistance can vary depending on the SLS. However, for most SLSs, the local windblown sand is defined as the volume of sedimented sand around an SMM or a railway component.

3 Modelling windblown sand around railways

In the following, we propose a probabilistic model to assess the windblown sand sedimented around railways by analogy with environmental actions in Civil Engineering [14], e.g. wind, windblown snow or wind-induced ice accretion.

3.1 Incoming windblown sand

Windblown sand results from the interaction of two physical subsystems, i.e. the wind and the sand. Among all transport mechanisms, saltation mainly contributes to the total transported sand mass [15]. In particular, windblown

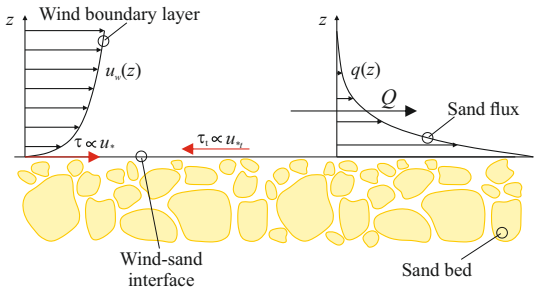

Fig. 4 Wind-sand interaction during saltation

sand saltation occurs when the wind shear velocity u_* is higher than the aeolian threshold shear velocity u_{*t} (Fig. 4).

The incoming windblown sand is defined as the amount of sand carried by the incoming wind undisturbed by any obstacle, in analogy to the incoming mean wind velocity in wind engineering practice. The resulting sand transport rate Q is defined as the integration of the sand flux q along the vertical direction. However, Q is usually estimated by means of semi-empirical models [15]. Such models are macroscopic constitutive laws that do not explicitly account for the variability of both wind and sand subsystems. The effects of the variability of the sand subsystem on u_{*t} have been investigated in a number of papers, reviewed in [16]. The evaluation of Q in a fully probabilistic approach is firstly introduced by [17], where both the variability of wind subsystem, i.e. speed and direction, and sand subsystem, i.e. aeolian threshold velocity, are taken into account. In this study, the following semi-empirical model is adopted [18]:

$$Q = 6.7\sqrt{\frac{d}{d_r}}\frac{\rho_a}{g}u_*^3\left(1-\frac{u_{*t}}{u_*}\right) \quad \text{if} \quad u_* > u_{*t} \tag{1}$$

$$Q = 0 \quad \text{if} \quad u_* \leq u_{*t} \tag{2}$$

where d_r=0.25 mm is the reference grain diameter, ρ_a is the air density, g is the acceleration of gravity.

3.2 Local windblown sand accumulation

The local sand accumulation is expressed by the time-cumulated sedimentation volume V. It is related to the incoming windblown sand by the sedimentation coefficient C_s. It depends on both the windblown sand yaw angle and the geometry of the obstacle, analogously to the aerodynamic coefficients in wind engineering. However, it is worth stressing a substantial difference: the obstacle is now described by a virtual geometry that varies over time and depends on the sedimentation volume. Given the lack of a closed form of C_s, its semi-empirical expression can be obtained by wind tunnel tests and/or computational simulations. Fig. 5a shows the conceptual scheme of the modelling

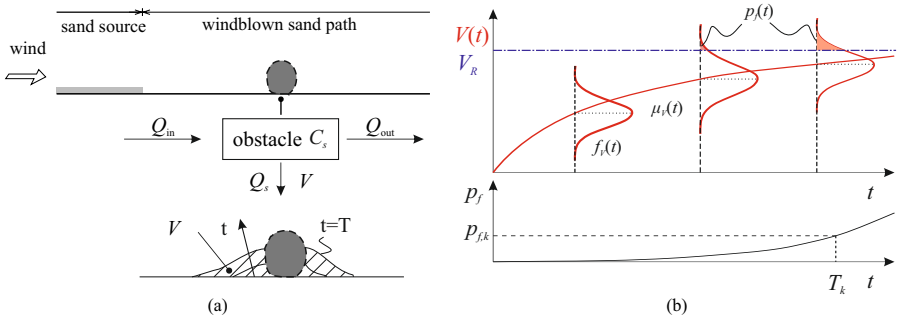

Fig. 5 Local windblown sand accumulation: conceptual scheme (a), time-variant sand volume and probability of failure (b)

framework. The incoming windblown sand Q_{in} splits into the sedimentation rate $Q_s = C_s Q_{in}$ and the outgoing transport rate $Q_{out} = (1 - C_s)Q_{in}$. The local accumulated sand volume V results from the time-cumulation of Q_s.
By analogy with common wind engineering practice, the incoming windblown sand direction is assumed in the worst case scenario, i.e. perpendicular to the obstacle. The generic obstacle splits the plane into two sides. As a result, the Probability Density Function (PDF) of Q_{in} derives from the side-PDF of the incoming wind speed, i.e. the non-directional PDF of the incoming wind speed from the left or the right side. The PDFs of Q_s and Q_{out} can therefore be obtained as

$$f(Q_s) = C_s(V) f(Q_{in}) \tag{3}$$

$$f(Q_{out}) = [1 - C_s(V)]\, f(Q_{in}) \tag{4}$$

Hence, the PDF of the accumulated sand volume can be obtained as the mixture of convolutions:

$$g(V) = \sum_{n=1}^{\infty} (f_1 * f_i * \ldots * f_n)\, Q_s P\,[N = n] \tag{5}$$

with $f_i = f$ for $i = 1, \ldots, N$, where $f(Q_s)$ is the probability density function of Q_s and N is the number of occurrences in which the wind blows in that direction over the reference time t. In order to assess the variables above, a Monte Carlo approach based on bootstrapping techniques from a dataset of observed wind values is adopted.
For a generic obstacle, a resistant sand volume can be defined according to a given SLS, e.g. the sand volume that leads to the overturning of a vertical wall for lateral earth pressure. In general, such a volume can be described by its nominal value V_R whatever the nature of the obstacle is. Indeed, its degree of uncertainty is much lower than the one of the sand volume. Hence, the basic condition for a satisfactory state [19] is:

$$V(t) < V_R \tag{6}$$

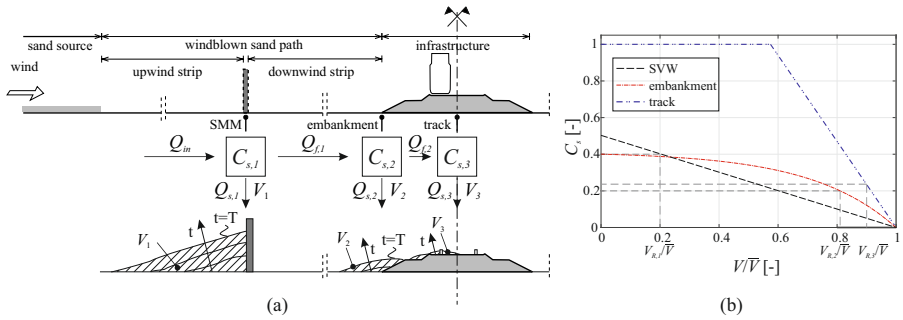

Fig. 6 Scheme of the setup geometry and related state variables (a), sedimentation coefficients versus filling ratios (b).

Fig. 5b shows the time-variant sand volume through its probability density function $f_V(t)$ and its mean value $\mu_V(t)$.
Given the nominal value V_R, the probability of failure $p_f(t)$ is equal to:

$$p_f(t) = P\left[V(t) > V_R\right] = 1 - F_V\left(V_R, t\right) \tag{7}$$

where F_V is the cumulative distribution of V. The characteristic failure time T_k can be defined as the time during which the condition (6) is violated only with a given probability $p_{f,k}$, i.e. $p_f(T_k) = p_{f,k}$. Assuming the monotonous function $V(t)$, p_f is also monotonous and its inverse function can be defined. Hence, the failure time can be derived as

$$T_k = p_f^{-1}\left(p_{f,k}\right) \tag{8}$$

4 Explorative application

In the following an effort is accomplished to put the proposed model at work aimed at demonstrating the technical feasibility of the approach in an engineering perspective.
The selected site is in the Arabian peninsula, along the North-South railway line. The railway alignment around the site develops along the West-East direction: it follows that the incoming sand transport rate Q_{in} attacks the railway from the North side and South side. The mean sand grain diameter is equal to d=0.35 mm. The aerodynamic roughness z_0 is equal to $z_0 = 4e-3$ m. The wind velocity in situ measurements refer to 6 years from Jan 2007 to Dec 2012. The 10-min average wind velocity U_{10} is recorded with a sampling yaw angle $\Delta\theta = 10°$ and a sampling time interval $\Delta t = 1$ hour. Fig. 6a shows the scheme of the setup geometry, and related state variables for a single side of the railway corridor. Such a scheme results directly from the general one in Fig. 5, by putting in series three obstacles, i.e. an SMM, the railway embankment, and the railway track. The same scheme holds for the opposite side of the railway. The height of the SMM and of the embankment are set equal to 4 m and 2.5 m, respectively. A double-track railway is considered, with a 0.25 m-width

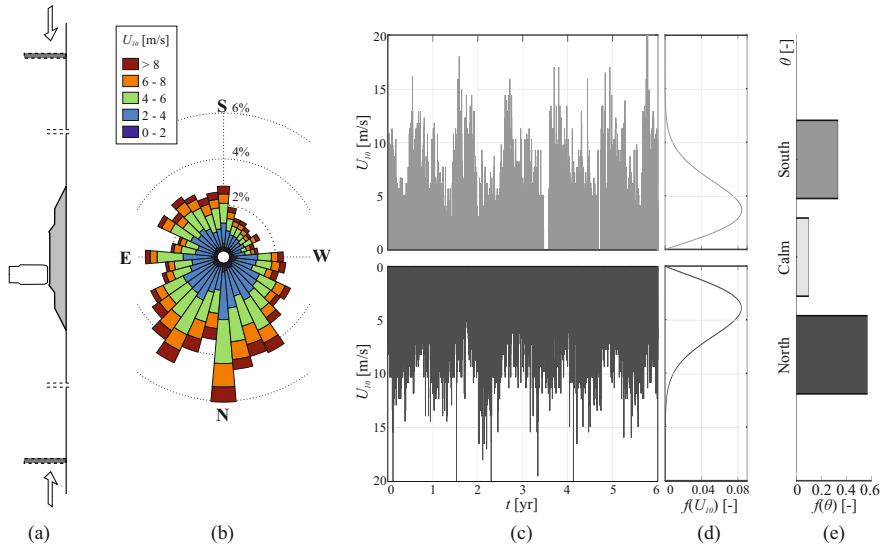

Fig. 7 Incoming wind statistics: setup geometry (a), wind rose (b), wind speed time histories (c), non-directional wind speed probability density functions (d), wind direction discrete probability density function (e).

ballast bed. The considered SMM is a common Straight Vertical Wall (SVW) [1]. The sedimentation coefficients C_s as a function of the dimensionless sedimented sand volume are plotted in Fig. 6b. They are obtained from [20]. Due to the lack of data on the railway track, its C_s is conjectured constant up to the filling of ballast voids (PVC=100%), and then linearly decreasing up to the maximum sedimented sand volume $\bar{V}$. The sand sedimented around the SMM and the embankment is planned to be removed when their sedimentation coefficients are lowered by 20% and 50%, respectively.

Both U_{10} and u_{*t} are random variables according to [17]. Monte Carlo simulation account for about 22e+6 realizations for each obstacle. The results discussed in the following refer to the attainment of SULS for full covering of the track under North winds only.

Fig. 7 shows the full wind rose (b), the time history of the non-directional wind speed incoming from both North and South railway sides (c), and the resulting statistics of both the wind speed U_{10} (d) and direction θ (e). $f(U_{10})$ is classically Weibull distributed. Fig. 8 gives an example of the framework at work, with regard to SVW and incoming wind from North side. For each obstacle: (a-c) plot 1-year long time histories of the incoming and filtered sand transport rate; (d-f) collect the realizations of the time-varying sedimented volume and related statistics, i.e. mean values μ and i-th percentiles p_{th}; (g-i) provide a close-up view of the PDF of the sedimented volume, the nominal sand resistance, the time varying resulting probability of failure, and the characteristic sand removal and failure times T_k corresponding to $p_{f,k}$=1%. The

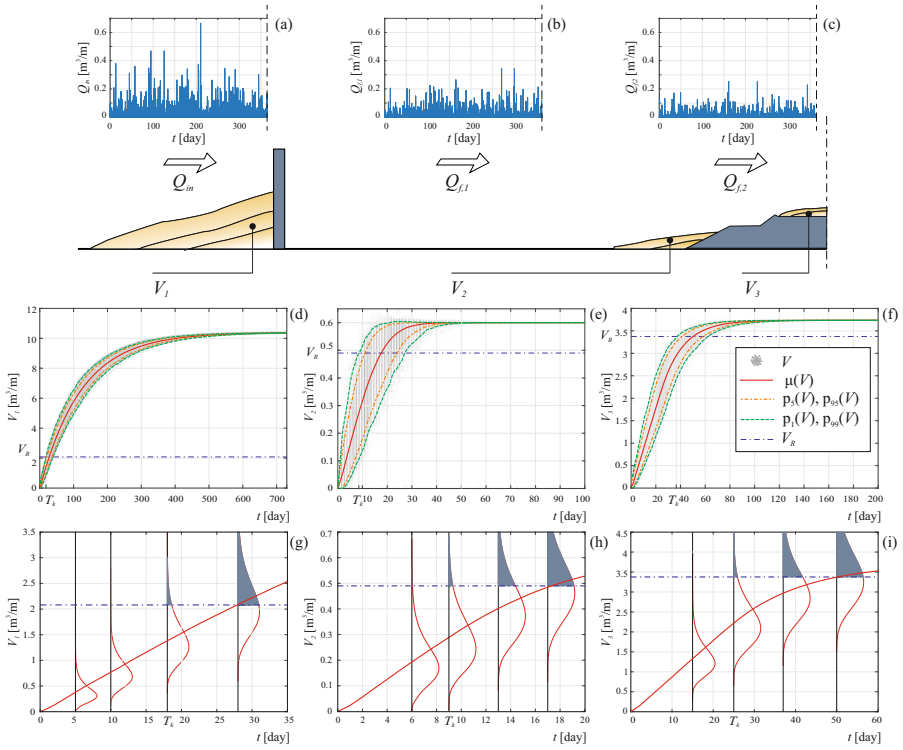

Fig. 8 Sedimented sand volume on SVW, embankment and track under North wind. Sand transport rate time histories (a-c) and time-variant accumulated volume (d-i).

sand transport rate is progressively reduced by in series obstacle filtering. The sedimented sand volume statistics for all obstacles share a horizontal asymptote at $\bar{V}_i$, while their trends depend on the sedimentation coefficient of each obstacle. The design value of the sand volume V_d corresponding to a target failure probability, e.g. $P_F \approx 10^{-6}$ for SULS, can be evaluated by the same proposed fully probabilistic approach, provided a large enough number of realizations are obtained. The corresponding sand removal and failure design times derives from eq. 7 and 8, i.e. $T_d = p_f^{-1}(P_F)$. The SULS partial safety factor γ can be derived a posteriori as $\gamma = V_d/V_k$ in a semi-probabilistic perspective.

5 Conclusions

We proposed the innovative probabilistic evaluation of the windblown sand accumulated volume on railways. The proposed framework allows evaluating sand removal and failure design times, and associated partial safety factors. The resulting safety format paves the way to the rationale design of sand

mitigation measures and sand removal planning from both the sand mitigation measures and railway tracks.

Acknowledgements The study has been developed in the framework of the Windblown Sand Modeling and Mitigation (WSMM) joint research, development and consulting group established between Politecnico di Torino and Optiflow Company. The authors wish to thank the other members of the WSMM group for the helpful discussions about the topics of the paper.

References

1. Bruno L., Fransos D., and Lo Giudice A. (2018). Solid barriers for windblown sand mitigation: Aerodynamic behavior and conceptual design guidelines, J. Wind Eng. Ind. Aerodyn. 173, 79–90.
2. EN 1990 (2002). Eurocode - Basis of structural design.
3. Bruno L., Horvat, M., and Raffaele L. (2018). Windblown sand along railway infrastructures: A review of challenges and mitigation measures, J. Wind Eng. Ind. Aerodyn. 177, 340-365.
4. Cheng J.j., Jiang F.q., Xue C.x., Xin G.w., Li K.c., and Yang Y.h. (2015). Characteristics of the disastrous wind-sand environment along railways in the Gobi area of Xinjiang, China. Atm. Env. 102, 344–354.
5. Nathawat V., and Sharda A. (2005) Challenges of Track Maintenance in Desert Area - Problems and Remedies. Permanent Way Bulletin. 32, 1–8.
6. Davel Wallis, M., 2014. Freight Train Derails. Namib Times.
7. Zakeri J.A., and Forghani M. (2012). Railway Route Design in Desert Areas. American Journal of Env. Eng. 2, 13–18.
8. Indraratna B., Su L., and Rujikiatkamjorn C. (2011). A new parameter for classification and evaluation of railway ballast fouling. Can. Geotech. J. 48, 322–326.
9. Ionescu D., Fedele D., Trounce M., and Petrolito J. (2016). Deformation and degradation characteristics of sand-contaminated railway ballast, in: Pombo, J. (Ed.), Proceedings of the Third International Conference on Railway Technology: Research, Development and Maintenance. Civil-Comp Press. Stirlingshire, UK.
10. Carrascal I., Casado J., Diego S., and Polanco J. (2016). Dynamic behaviour of high-speed rail fastenings in the presence of desert sand. Constr. Building Mat. 117, 220-228.
11. Faccoli M., Petrogalli C., Lancini M., Ghidini A., and Mazzù A. (2018). Effect of desert sand on wear and rolling contact fatigue behaviour of various railway wheel steels. Wear. 396-397, 146–161.
12. Tyfour, W. R., 2008. Predicting the effect of grinding corrugated rail surface on the wear behavior of pearlitic rail steel. Tribol. Lett. 29, 229–234.
13. Kóllmann, J., 2013. Railway operations under harsh environmental conditions sand, dust & humidity problems and technical solutions/mitigation measures. In: AHK Workshop Be a Partner of Qatar Rail, Berlin.
14. EN 1991 (2003). Eurocode 1: Actions on structures.
15. Kok J.F., Parteli E.J.R., Michaels T.I., and Karam D.B. (2012). The physics of wind-blown sand and dust. Rep. Prog. Phys. 75.
16. Raffaele L., Bruno L., Pellerey F., and Preziosi L. (2016). Windblown sand saltation: A statistical approach to fluid threshold shear velocity. Aeolian Res. 23, 79-91.
17. Raffaele L., Bruno L., Fransos D., and Pellerey F. (2017). Incoming windblown sand drift to civil infrastructures: A probabilistic evaluation. J. Wind Eng. Ind. Aerodyn. 166, 37-47.
18. Lettau K., and Lettau H. (1987). Experimental and micro-meteorological field studies of dune migration. Exploring the World's Driest Climate (IES Report). 101, 110-147.
19. Melcher E. R., and Beck A. T. (2018). Structural Reliability Analysis and Prediction. Wiley.
20. Hotta S., and Horikawa K. (1990). Function of sand fence placed in front of embankment. In: Coastal Engineering, American Society of Civil Engineers, New York, USA.